34th Annual International Conference of the IEEE EMBS
San Diego, California USA, 28 August - 1 September, 2012

Modeling Normal and Rebound Excitation in Mammalian Retinal Ganglion Cells

Tianruo Guo , *Student Member, IEEE,* David Tsai , *Member, IEEE,* Gregg J. Suaning, *Member, IEEE*, Nigel H. Lovell , *Fellow, IEEE and* Socrates Dokos , *Member, IEEE*

***Abstract*— In this study, we used a novel missing currents technique to extend an existing conductance-based ionic current model of retinal ganglion cells (RGCs). The revised model reproduced a variety of biological behaviors. In particular, the model contains a hyperpolarization activated current (I_h). This model can effectively simulate the mechanisms underlying both normal and rebound action potentials. The technique used in this study is generally applicable to other excitable cell models, reducing the gap between theoretical models and real biological neurons.**

I. Introduction

Elucidation of ionic mechanisms underlying retinal ganglion cell (RGC) electrical activity is important for the development of effective stimulation strategies in prosthetic vision implants. Mathematical models can integrate the experimental information and biophysical principles into a systematic mechanistic understanding of electrophysiology, predicting biological information hidden in the data, as well as effectively utilizing available information to improve existing knowledge. Over the past several decades, computational models have become increasingly important for an integrative understanding of underlying ionic mechanisms in neuron electrophysiology. Existing ionic models have been able to reconstruct neuronal electrical activity to some extent [1-6]. However, their abilities to simultaneously reproduce RGC electrophysiological behaviors under a large range of different experimental conditions, is still unclear. Rebound excitation, also termed post-inhibitory rebound, had been studied in a number of neuron types, [2, 7, 8]. To our knowledge, only a limited number of existing ionic models can effectively reproduce such phenomena.

It is therefore desirable to develop computationally simple, robust parameter optimization approaches along with corresponding ionic models, which can accurately simulate multiple electrophysiological mechanisms in RGCs. By optimizing the appropriate model parameters, the same model should be able to fit multiple experimental data recorded under different experimental conditions. With desired experimental designs, such a model should be able to reproduce complex behaviors such as normal and rebound membrane voltage responses due to variable current injections.

In this study, a modified rabbit RGC ionic model, based on the Fohlmeister and Miller (FM) formulation (1997) [1], was optimized to simultaneously reproduce multiple RGC electrophysiological behaviors. An additional ionic current, which exhibited a significant response to hyperpolarizing current injection, was present in the model to simulate mechanisms underlying rebound action potentials.

Tianruo Guo, David Tsai, Gregg J. Suaning, Nigel H. Lovell and Socrates Dokos are with the Graduate School of Biomedical Engineering, University of New South Wales, Sydney, 2052, Australia. (e-mail: s.dokos@unsw.edu.au).

II. Methodology

A. RGC Model

The RGC model used in this study consisted of six time-dependent ionic currents and one leakage current. Besides the formulations included in the FM model, one current, hyperpolarization-activated current (I_h) was added to fit the potential missing currents which were absent in the original model structure.

$$\frac{dE_m}{dt} = -\frac{1}{C_m}\left(J_{ion} + J_{mis}\right)$$

$$J_{mis} = I_h \qquad (1)$$

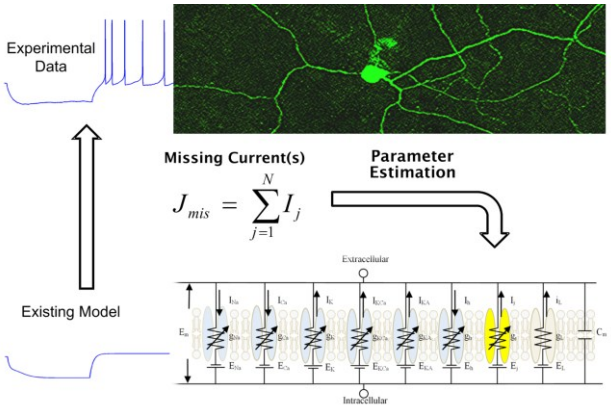

Figure. 1. Missing currents fitting process. Modified model structure (J_{mis}) will depend on the information provided by extra experimental data and multiple model outputs. The model results are compared against experimental data to extract the missing current(s). A revised model incorporating these additional currents is constructed and optimized to minimize the difference between model outputs and cell responses.

TABLE I.
RATES OF VOLTAGE-GATED IONIC CHANNEL

Channel	Rate Function
I_h	$\alpha_y = k_\alpha e^{S_\alpha (E_m - E_{50,\alpha})}$ $\beta_y = \frac{k_\beta (E_m - E_{50,\beta})}{1 - e^{S_\beta (E_m - E_{50,\beta})}}$

where J_{ion} and J_{mis} are the FM currents and missing current respectively. I_h was described by standard Hodgkin-Huxley schemes:

$$I_h = g_h \cdot y^2 \cdot (E_m - E_h) \quad (2)$$

where g_h is the maximum conductance of the missing current, and gating variables y satisfy first order ODEs:

$$\frac{dy}{dt} = \alpha_y (1 - y) - \beta_y y \quad (3)$$

where α_y , β_y are the opening and closing rates respectively. The mathematical description of each rate can be found in Table I.

B. Missing Currents Fitting Technique

A missing current fitting technique was used to identify the potential missing currents absent in the existing ionic model. The modified model structure will depend on the information provided by extra experimental data and multiple model outputs. In this study, for example, results from the original FM model suggested that additional ionic currents activated by hyperpolarization, are necessary for reproducing rebound excitation (see Fig. 1). Parameter values were estimated by minimizing the sum of squares of the difference between the multiple experimental data and corresponding model outputs, using a custom curvilinear gradient-based optimization method [9]. Rather than only tuning the missing current (8 parameters), the original FM model (46 parameters) were also optimized. Model parameters across these multiple datasets were constrained to share the same values since any action potential waveshape variation would be due to differences in the external stimulus current alone. The optimization process was performed on a standard desktop PC using Matlab (The Mathworks Inc.).

C. Experimental Methods

All procedures were approved and monitored by the University of New South Wales Animal Care and Ethics Committee. The procedures have been described in detail previously [10]. Briefly, New Zealand White rabbits weighing 2.0 ~ 3.0 kg were anesthetized with Ketamine (70 mg/kg) + Xylazine (10 mg/kg). After enucleating an eye, the animal was euthanized with sodium pentobarbital. The eye was hemisected, the anterior portion discarded and the vitreous cleared. Small pieces of the inferior retina, with the sclera attached, were dissected and kept in Ames' medium

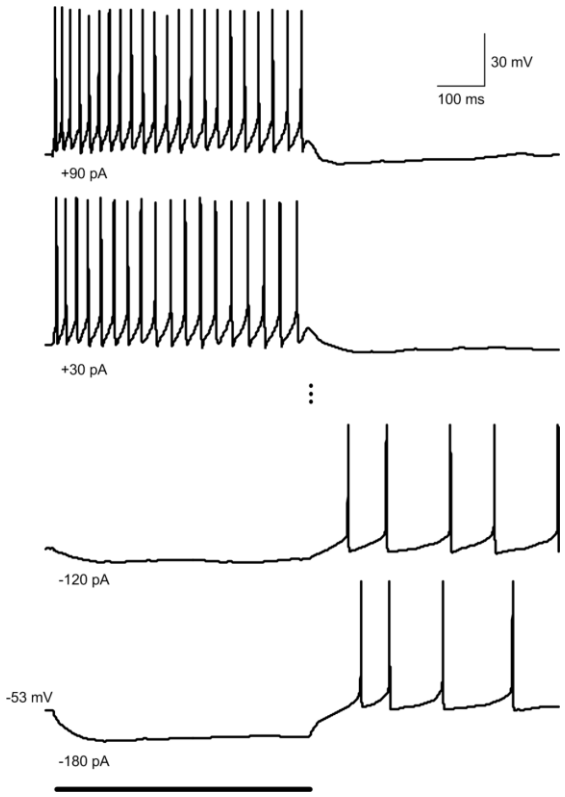

Figure. 2. Depolarizing and hyperpolarizing responses of biological RGC while injecting a family of current pulses (500 ms duration, -180 ~ 120 pA, in 30 pA steps) via the patch electrode.

equilibrated with 95% O_2 / 5% CO_2, supplemented with 1% Penicillin/Streptomycin at room temperature in darkness. Before electrophysiological recordings, a small piece of the retina was separated from the pigment epithelium and sclera and transferred RGC-side up into an imaging chamber. The retinas were perfused with equilibrated Ames medium at ~ 5 mL / min and heated to 34 ~ 35 ˚C throughout the recording period. RGCs in the whole-mount retina were visualized and targeted for recording with near-IR illumination.

We performed whole-cell current clamp recordings from the RGCs (N=100) using glass electrodes filled with (mM): 116 $KMeSO_4$, 10 KCl, 0.008 $CaCl_2$, 0.7 EGTA, 1 $MgCl_2$, 10 HEPES, 4 ATP-Na_2, 0.5 GTP-Na_3, 0.075 Alexa Fluor 488, and 10 Neurobiotin-Cl, pH 7.2. Electrode resistances ranged from 3.0 ~ 5.0 MΩ. Series tip resistance was compensated accordingly on the amplifier (MultiClamp 700B, Molecular Devices). Data were low-pass filtered at 10 kHz and digitized at 50 kHz on a computer running pClamp 10 (Molecular Devices). All data were analyzed in pClamp 10 and Matlab R2010a (Mathworks).

We blocked all RGC excitatory (AMPA/kainate, NMDA and mGluR6) and inhibitory ($GABA_{a/c}$ and glycine) synaptic inputs by bath application of a mixture containing (μM): 75 6-cyano-7-nitroquinoxaline-2, 3-dione (CNQX), 60 (+)-MK 801 hydrogen maleate, 20 L-(+)–2–Amino–4-phosphonobutyric acid (L-AP4), 100 picrotoxin and 10 strychnine. All blockers were supplied by Tocris Bioscience

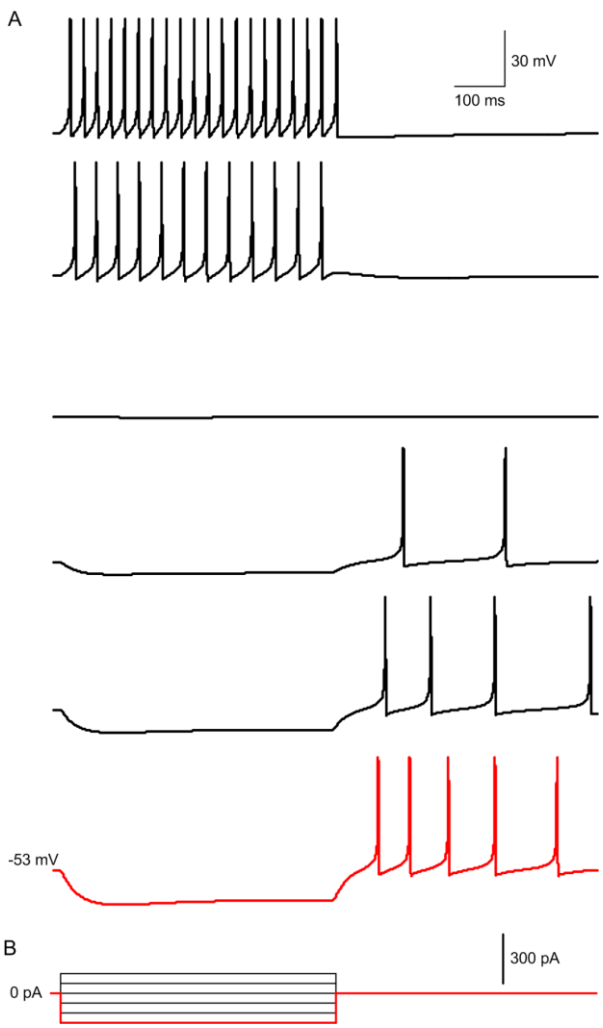

Figure. 3. A. Multiple model-generated membrane potentials in response to various somatic current injections: The model reproduced both normal and rebound RGC spikes. B. External stimuli: 500 ms somatic current injection from -180 pA (red line) to 120 pA, in 60 pA steps.

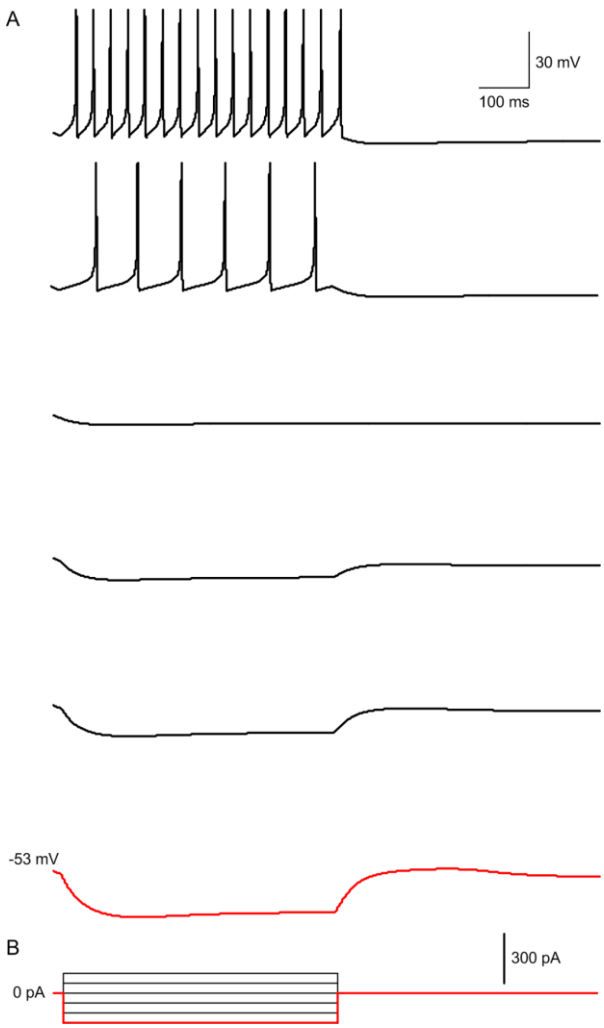

Figure. 4. A. Multiple model-generated membrane potentials after I_h was partly blocked. The rebound membrane potentials (lower three panels) were eliminated by reducing the maximum conductance of I_h by 30%, whilst the depolarized (upper two panels) and spontaneous (third panel) activities were relatively unaltered. B. Somatic current step.

and Sigma Aldrich.

III. Results

A. RGC Depolarization and Hyperpolarization

Voltage responses from an RGC were recorded during depolarizing and hyperpolarizing somatic current injections. The results shown in Fig. 2 demonstrate a slow depolarizing "sag" on hyperpolarization below resting membrane potential, and a significant rebound excitation after hyperpolarization. In addition, both normal and rebound action potentials exhibited significant frequency adaptation. Further increases in the amplitude of both depolarized and hyperpolarized current injections led to an increase in the spike frequency.

B. Model Results

The RGC model was optimized to simultaneously fit voltage responses stimulated by both depolarizing and hyperpolarizing currents (-180 and 120 pA). Estimated parameters across these two datasets were specified to share the same values since any AP waveshape variation would be due to differences in the injected current alone. A total of six time-dependent ionic currents and one leakage current were used to reproduce the multiple datasets. From the results shown in Fig. 3A, the model outputs can closely match the experimental data from Fig. 2, including the slow depolarizing "sag" on hyperpolarization below resting membrane potential, a significant rebound excitation after hyperpolarization, as well as corresponding spike frequency and first spike latency (FSL) variation due to stimulus amplitude. It should be noticed that the optimized model could also effectively predict datasets which were not used in the optimization process by tuning the stimulus amplitude (i.e. -120, -60, 0 and 60 pA).

C. Blockage of Hyperpolarization-Activated Current

An additional simulation was undertaken to investigate the contribution of the hyperpolarization-activated current in our

modified RGC model. One data-specific parameter, g_h, the maximum conductance of I_h, was reduced by 30%, in order to model the effect of I_h on rebound excitation in the RGC. All other model parameters were held fixed. As shown in Fig. 4A, the rebound impulse can be obviously eliminated when I_h was partially blocked by reducing its maximum conductance, while the depolarized voltage responses were relatively unaltered. In addition, blockage of I_h resulted in shifting of resting membrane potential.

IV. Discussion and Conclusion

Recently published modeling work has given more attention to the mechanisms underlying rebound excitation in different types of neurons [2, 4, 5]. In this study, a major improvement over existing modeling approaches was that large-scale optimization was performed on all model parameters rather than only maximum membrane conductances. We believe that estimating only membrane conductances while fixing ion channel kinetics parameters will excessively limit the parameter search space, reducing the accuracy of model fits, particularly when optimizing against multiple datasets. In this study all models were optimized to closely reproduce action potential waveforms recorded under multiple current injections, which would not be possible if limited to optimizing only the few membrane conductance parameters available. In addition, our multi-dataset optimized parameters yielded good predictions to non-optimized data. We believe that this will be generally hard to achieve with only single-dataset optimization.

The contribution of I_h to neuronal excitability has been reported in many studies [11-13]. In our results, rebound excitation can be eliminated when I_h is blocked by partially reducing its maximum conductance, revealing its contribution to the rebound excitation in RGCs. Also, our results indicated that I_h may contribute to the resting membrane properties of RGC. Indeed, the range of resting potential of RGC can be within activation range of I_h. It should be noted that not only I_h is responsible for rebound excitation. Many studies have reported that low voltage activated calcium current and persistent sodium current can also have significant contribution to rebound excitation [5, 6, 14]. One of our future refinements of this work will be modifying the model by adding other identified missing currents.

The predicted results to non-optimized data could help in refining experimental designs for obtaining additional data, which in turn may modify the model structure (e.g. by continually incorporating additional ionic currents into the model) or parameters (e.g. by limiting or relaxing constraints on certain model parameters to reproduce new experimental information). A positive coupling between simulation and experiment can be achieved by iteratively comparing model-predicted results and subsequent experimental data. This missing currents fitting technique is generally applicable to other excitable cell models. By using this technique, more accurate ionic models can be constructed semi-automatically, reducing the gap between theoretical models and real biological neurons.

Acknowledgment

This research was supported by Australia Research Council (ARC) through its Special Research Initiative (SRI) in Bionic Vision Science and technology grant to Bionic Vision Australia (BVA).

References

[1] J. F. Fohlmeister and R. F. Miller, "Impulse encoding mechanisms of ganglion cells in the tiger salamander retina," *J. Neurophysiol.,* vol. 78, pp. 1935-1947, 1997.

[2] T. B. Kepler, L. F. Abbott, and E. Marder, "Reduction of conductance-based neuron models," *Biol. Cybern.,* vol. 66, pp. 381-7, 1992.

[3] G. Wainrib, M. Thieullen, and K. Pakdaman, "Reduction of stochastic conductance-based neuron models with time-scales separation," *J. Comput. Neurosci.,* vol. 32, 2011.

[4] F. Buchholtz, J. Golowasch, I. R. Epstein, and E. Marder, "Mathematical model of an identified stomatogastric ganglion neuron," *J. Neurophysiol.,* vol. 67, pp. 332-40, 1992.

[5] T. Kameneva, H. Meffin, and A. N. Burkitt, "Modelling intrinsic electrophysiological properties of ON and OFF retinal ganglion cells," *J. Comput. Neurosci.,* vol. 31, pp. 547-61, 2011.

[6] D. A. McCormick and J. R. Huguenard, "A model of the electrophysiological properties of thalamocortical relay neurons," *J. Neurophysiol.,* vol. 68, pp. 1384-400, 1992.

[7] P. Mitra and R. F. Miller, "Normal and rebound impulse firing in retinal ganglion cells," *Vis. Neurosci.,* vol. 24, pp. 79-90, 2007.

[8] P. Mitra and R. F. Miller, "Mechanism underlying rebound excitation in retinal ganglion cells," *Vis. Neurosci.,* vol. 24, pp. 709-31, 2007.

[9] S. Dokos and N. H. Lovell, "Parameter estimation in cardiac ionic models," *Prog. Biophys. Mol. Biol.,* vol. 85, pp. 407-431, 2004.

[10] D. Tsai, J. W. Morley, G. J. Suaning, and N. H. Lovell, "Frequency-dependent reduction of voltage-gated sodium current modulates retinal ganglion cell response rate to electrical stimulation," *J. Neural. Eng.,* vol. 8, p. 066007, 2011.

[11] Y. Rateau and N. Ropert, "Expression of a functional hyperpolarization-activated current (Ih) in the mouse nucleus reticularis thalami," *J. Neurophysiol.,* vol. 95, pp. 3073-85, 2006.

[12] S. Moosmang, J. Stieber, X. Zong, M. Biel, F. Hofmann, and A. Ludwig, "Cellular expression and functional characterization of four hyperpolarization-activated pacemaker channels in cardiac and neuronal tissues," *Eur. J. Biochem.,* vol. 268, pp. 1646-52, 2001.

[13] A. Momin, H. Cadiou, A. Mason, and P. A. McNaughton, "Role of the hyperpolarization-activated current Ih in somatosensory neurons," *J. Physiol.,* vol. 586, pp. 5911-29, 2008.

[14] X. J. Wang, J. Rinzel, and M. A. Rogawski, "A model of the T-type calcium current and the low-threshold spike in thalamic neurons," *J. Neurophysiol.,* vol. 66, pp. 839-50, 1991.